

RNA-sequencing analysis reveals new alterations in cardiomyocyte cytoskeletal genes in patients with heart failure

Isabel Herrer¹, Esther Roselló-Lletí¹, Miguel Rivera¹, María Micaela Molina-Navarro¹, Estefanía Tarazón¹, Ana Ortega¹, Luis Martínez-Dolz², Juan Carlos Triviño³, Francisca Lago⁴, José R González-Juanatey⁴, Vicente Bertomeu⁵, José Anastasio Montero⁶ and Manuel Portolés¹

Changes in cardiomyocyte cytoskeletal components, a crucial scaffold of cellular structure, have been found in heart failure (HF); however, the altered cytoskeletal network remains to be elucidated. This study investigated a new map of cytoskeleton-linked alterations that further explain the cardiomyocyte morphology and contraction disruption in HF. RNA-Sequencing (RNA-Seq) analysis was performed in 29 human LV tissue samples from ischemic cardiomyopathy (ICM; $n = 13$) and dilated cardiomyopathy (DCM, $n = 10$) patients undergoing cardiac transplantation and six healthy donors (control, CNT) and up to 16 ICM, 13 DCM and 7 CNT tissue samples for qRT-PCR. Gene Ontology analysis of RNA-Seq data demonstrated that cytoskeletal processes are altered in HF. We identified 60 differentially expressed cytoskeleton-related genes in ICM and 58 genes in DCM comparing with CNT, hierarchical clustering determined that shared cytoskeletal genes have a similar behavior in both pathologies. We further investigated *MYLK4*, *RHOA*, and *ANKRD1* cytoskeletal components. qRT-PCR analysis revealed that *MYLK4* was downregulated (-2.2 -fold; $P < 0.05$) and *ANKRD1* was upregulated (2.3 -fold; $P < 0.01$) in ICM patients vs CNT. *RHOA* mRNA levels showed a statistical trend to decrease (-2.9 -fold). In DCM vs CNT, *MYLK4* (-4.0 -fold; $P < 0.05$) and *RHOA* (-3.9 -fold; $P < 0.05$) were downregulated and *ANKRD1* (2.5 -fold; $P < 0.05$) was upregulated. Accordingly, MYLK4 and ANKRD1 protein levels were decreased and increased, respectively, in both diseases. Furthermore, *ANKRD1* and *RHOA* mRNA levels were related with LV function ($P < 0.05$). In summary, we have found a new map of changes in the ICM and DCM cardiomyocyte cytoskeleton. *ANKRD1* and *RHOA* mRNA levels were related with LV function which emphasizes their relevance in HF. These new cytoskeletal changes may be responsible for altered contraction and cell architecture disruption in HF patients. Moreover, these results improve our knowledge on the role of cytoskeleton in functional and structural alterations in HF.

Laboratory Investigation (2014) 94, 645–653; doi:10.1038/labinvest.2014.54; published online 7 April 2014

KEYWORDS: ANKRD1; cytoskeleton; heart failure; left ventricular function; MYLK4; RHOA; RNA-Seq

Heart failure (HF) is a syndrome in which the heart cannot pump enough blood to meet the needs of the body.¹ The main factors implicated in HF have been associated with neuroendocrine abnormalities, re-expression of fetal genes, alterations in the energetic state of the myocyte, and changes in the contraction process that result in impaired cardiac function.^{2,3} These functional alterations have a structural basis involving cellular and interstitial changes that manifest as differences in size, shape, and extracellular matrix

properties.⁴ These morphological alterations have been proposed to occur in response to injury or stress stimulus and may be an adaptive response to overcome depressed cardiac function.

As a key regulator of cellular architecture, cardiomyocyte cytoskeletal components also have an active role in contraction and relaxation processes and intracellular signaling.^{2,5} The cytoskeleton of myocytes includes cytoskeletal proteins such as tubulin or actin, as well as their membrane-associated

¹Cardiocirculatory Unit, IIS La Fe, Valencia, Spain; ²Cardiocirculatory Unit, IIS La Fe, Hospital Universitario LA FE, Valencia, Spain; ³Genomic System, Valencia, Spain; ⁴Cardiology Unit, Hospital Clínico Santiago Compostela, La Coruña, Spain; ⁵Cardiology Unit, Hospital Universitario San Juan, Alicante, Spain and ⁶Cardiovascular Surgery Service, Hospital Universitario La Fe, Valencia, Spain
Correspondence: Dr M Portolés Sanz, PhD, Cardiocirculatory Unit, IIS La Fe, Hospital Universitario LA FE, Avenida Campanar 21, 46009 Valencia, Spain.
E-mail: portoles_man@gva.es

Received 7 November 2013; revised 12 February 2014; accepted 26 February 2014

proteins, the sarcomere, and the myofibrillar stretch-sensor system. Alterations in proteins of the cytoskeleton have been demonstrated in both animal models and in humans in cardiac hypertrophy and HF.^{6–8} The major alterations described in the failing heart are changes in the sarcomeric skeleton, in combination with the loss of contractile filaments, and changes in the regulatory proteins of myofibrils that alter their phosphorylation status. A compensatory response represented by an increase in cytoskeletal proteins (tubulin family members and desmin) and membrane-associated proteins was also described and may contribute to the decrease in stability and integrity of myocytes in failing hearts.⁹ Other studies determined a role of cell Z-disc components in chamber dilation, suggesting that the interface of the cytoskeleton and the sarcomere are critical for the development of cardiomyopathy.¹⁰ Furthermore, other studies proposed that cytoskeletal alterations are responsible enough for the initiation of some types of HF, such as dilated cardiomyopathy (DCM).¹¹ Interfering with changes in some cytoskeletal proteins causes improved cardiac function; therefore, it has been suggested to be a potential therapeutic target.¹²

Despite all these studies, an accurate analysis of such complex networks requires global gene-expression approaches. Advances in molecular biology and the development of microarray technology have allowed global gene-expression profiling analysis, and the identification of signaling pathways that contribute to various aspects of HF.^{13,14} Previous studies using this technical approach identified changes in the expression levels of genes related to cytoskeletal function in human HF;¹⁵ however, many cytoskeleton and effector genes have not been discussed yet using high-throughput sequencing technologies. RNA-sequencing (RNA-Seq) technology provides a more precise and sensitive method to map and quantify RNA transcripts compared with the analog data generated by microarray technology.¹⁶

We hypothesized that HF patients may undergo new changes in cytoskeletal genes not described yet using conventional mRNA analysis techniques. These alterations may participate in cardiomyocyte structure disruption as well as contraction defects. Therefore, the aim of this study was to highlight a select group of cytoskeletal genes and effectors using RNA-Seq in patients with ischemic cardiomyopathy (ICM) and non-ischemic DCM in comparison with control subjects (CNT), and find out their functional relationship.

MATERIALS AND METHODS

Tissue Collection

Left ventricular (LV) tissue samples were collected from human hearts obtained from 13 and 16 patients with ICM, and 10 and 13 patients with DCM undergoing cardiac transplantation, and subsequently used in RNA-Seq or qRT-PCR, respectively. ICM was diagnosed on the basis of the clinical history, Doppler echocardiography, and coronary angiography data. Non-ischemic DCM was diagnosed when patients had

LV systolic dysfunction (ejection fraction (EF) < 40%) with a dilated non-hypertrophic LV (LV diastolic diameter (LVDD) > 55 mm) on echocardiography. Moreover, patients did not show existence of primary valvular disease and familial DCM. The clinical characteristics of the patients are shown in Table 1, which includes more detailed data. All patients were functionally classified according to the New York Heart Association (NYHA) criteria and were receiving medical treatment following the guidelines of the European Society of Cardiology.¹⁷

CNT LV samples were obtained from the hearts of six (RNA-Seq) or seven (qRT-PCR) healthy donors whose hearts could not be transplanted due to surgical reasons or blood-type incompatibility. The cause of death in these individuals was cerebrovascular or motor vehicle accident. All donors had normal LV function and had no history of myocardial disease or active infection at the time of transplantation.

Fresh transmural samples were recovered from near the apex of the left ventricle at the time of transplantation and maintained in 0.9% NaCl after the extraction procedure. Tissue samples are stored at 4 °C for a maximum of 6 h from the time of coronary circulation loss and then frozen at – 80 °C.

Table 1 Patient characteristics according to HF etiology (RNA-Seq)

	ICM (n = 13)	DCM (n = 10)
Age (years)	54 ± 7	54 ± 9
Gender male (%)	100	90
NYHA class	3.5 ± 0.4	3.3 ± 0.3
BMI (kg/m ²)	26 ± 4	27 ± 7
Hemoglobin (mg/ml)	14 ± 3	13 ± 3
Hematocrit (%)	41 ± 6	39 ± 8
Total cholesterol (mg/dl)	162 ± 41	139 ± 30
Prior hypertension (%)	30	11
Prior smoking (%)	84	22
Prior diabetes mellitus (%)	38	18
EF (%)	24 ± 4*	18 ± 6
FS (%)	13 ± 2*	10 ± 3
LVEDD (mm)	55 ± 7*	68 ± 12
LVEDD (mm)	64 ± 7*	76 ± 11
LV mass (g)	262 ± 68*	434 ± 111

Abbreviations: BMI, body mass index; DCM, dilated cardiomyopathy; EF, ejection fraction; FS, fractional shortening; HF, heart failure; ICM, ischemic cardiomyopathy, LVEDD, left ventricular end-diastolic diameter; LVESD, left ventricular end-systolic diameter; LVm, left ventricular mass; NYHA, New York Heart Association; RNA-seq, RNA-Sequencing.

Data are showed as the mean value ± s.d. **P* < 0.05 significantly different between DCM and ICM patients.

This study has been approved by the Ethics Committee of Hospital la Fe in accordance with the guidelines of the Declaration of Helsinki.¹⁸ Informed written consent has been obtained from each patient before tissue collection.

RNA Extraction

Heart tissues were homogenized with TRIzol reagent in a TissueLyser LT apparatus (Qiagen, Manchester, UK). All RNA extractions were performed using a PureLink Kit according to the manufacturer's instructions (Ambion, Life Technologies, Foster City, CA, USA). RNA was quantified using a NanoDrop1000 spectrophotometer (Thermo Fisher Scientific, Loughborough, UK), and the purity and integrity of RNA samples were measured using an Agilent 2100 Bioanalyzer with the RNA 6000 Nano LabChip kit (Agilent Technologies, Madrid, Spain). All samples displayed a 260/280 ratio ≥ 2.0 , and RNA integrity numbers were ≥ 9 .

RNA-Seq

RNA samples were isolated using the MicroPoly(A) Purist kit (Ambion). Total PolyA-RNA was used to generate whole-transcriptome libraries for sequencing on the SOLiD 5500XL platform following the manufacturer's recommendations (Life Technologies). Amplified cDNA quality was analyzed using the Bioanalyzer 2100 DNA 1000 kit (Agilent Technologies) and quantified using the Qubit 2.0 Fluorometer (Invitrogen, Paisley, UK). The whole-transcriptome libraries were used for making SOLiD templated beads following the SOLiD Templated Bead Preparation guide. This protocol comprised a clonal amplification step following an enrichment and chemical modification process. Bead quality was estimated on the basis of workflow analysis (WEA) parameters. The samples were sequenced using the 50625 paired-end protocol, generating 75 nt + 35 nt (Paired-End) + 5 nt (Barcode) sequences. Quality data were measured using SOLiD Experimental Tracking System software parameters.

Computational Analysis of RNA-Seq Data

The initial whole-transcriptome paired-end reads obtained from sequencing were mapped against the latest version of the human genome (version GRchr37/hg19) using the Life Technologies mapping algorithm (<http://www.lifetechnologies.com/>). The aligned records were reported in BAM/SAM format.

Insufficient quality reads (phred score < 10) were eliminated using the Picard Tools software. Gene prediction was estimated using the cufflinks method,¹⁹ and the expression levels were calculated using the HT Seq software.

Differential expression analysis between conditions was performed using the Edge method. This method relies on a Poisson model to estimate the variance in the RNA-Seq data for differential expression. Finally, we selected differentially expressed genes with a P -value < 0.05 and a fold change of at least 1.5.

Gene Functional Annotation

Functional analysis of differentially expressed genes was performed using the Database for Annotation, Visualization and Integrated Discovery (DAVID, version 6.7). We selected the gene ontology (GO) terms that had a P -value < 0.05 .

Clustering Analysis

Relative mRNA expression levels obtained from RNA-Seq data of cytoskeletal selected genes were represented in an interval of ± 5 . Hierarchical clustering with squared Euclidean distance was applied to identify gene clusters.

RNA-Seq Validation using qRT-PCR

Onemicrogram of RNA was reverse-transcribed to cDNA using the M-MLV enzyme (Invitrogen). qRT-PCR assays were performed in duplicate using TaqMan technology in the ViiA7 Fast Real-Time RT-PCR System according to the manufacturer's instructions (Applied Biosystems, Foster City, CA, USA). All TaqMan probes were designed and obtained from Applied Biosystems. Myosin light chain kinase family, member 4 (*MYLK4*, *Hs01584163_m1*), ras homolog family member U (*RHOU*, *Hs00221873_m1*), and ankyrin repeat domain 1 gene (*ANKRD1*, *Hs00173317_m1*). Housekeeping genes *GAPDH* (*Hs99999905_m1*), *PGK1* (*Hs99999906_m1*), and *TFRC* (*Hs00951083_m1*) were used as reference. To determine transcript quantity, $\Delta\Delta C_t$ -based fold-change calculations were used.²⁰

Homogenization of Samples, Electrophoresis, and Western Blot Analysis

Thirty micrograms of frozen left ventricles were minced and mechanically disrupted. Tissue samples were then transferred into Lysing Matrix D tubes designed for use with the FastPrep-24 homogenizer (MP Biomedicals, Madrid, Spain) in total protein extraction buffer (2% SDS, 10 mM EDTA, 6 mM Tris-HCl, pH 7.4) with protease inhibitors (25 $\mu\text{g}/\text{ml}$ aprotinin and 10 $\mu\text{g}/\text{ml}$ leupeptin). Tissue debris are removed by centrifugation and supernatants were collected. Protein quantification was determined using Peterson's modification of the micro Lowry method, using bovine serum albumin as a standard.

Protein samples were separated by Bis-Tris electrophoresis on 4–12% polyacrylamide gels and transferred to a PVDF membrane using the iBlot Gel Transfer Device (Invitrogen) for western blot analyses. The primary detection antibodies used were anti-MYLK4 rabbit polyclonal (1:250), anti-ANKRD1 rabbit polyclonal (1:200), and anti-WRCH1 rabbit polyclonal (1:1000) antibodies. Monoclonal anti-GAPDH antibody (1:10 000) was used as a loading control. All antibodies were from Abcam (Cambridge, UK), except Anti-ANKRD1, which was obtained from Santa Cruz Biotechnology (Santa Cruz, CA, USA).

Bands were visualized using an acid phosphatase-conjugated secondary antibody and nitro blue tetrazolium/5-bromo-4-chloro-3-indolyl phosphate (NBT/BCIP, Sigma,

Saint Louis, MO, USA) substrate system. Finally, the bands were digitalized using an image analyzer (DNR Bio-Imaging Systems, Jerusalem, Israel) and quantified by the GelQuant Pro (v12.2) program.

Statistics

Data are expressed as means \pm s.d.'s. Kolmogorov–Smirnov test was applied to evaluate the data distribution. Comparisons of clinical characteristics were achieved using Student's *t*-test for continuous variables and Fisher's exact test for discrete variables. Student's *t*-test was used to determine significant mean differences in mRNA and protein levels between groups, and the nonparametric Mann–Whitney *U*-test was performed for data that were not normally distributed. To study the relationship between mRNA expression levels and clinical parameters, we used bivariate correlation analysis. Pearson's correlation coefficient was calculated to analyze the association between normal variables and Spearman's for not normally distributed data. Significance was defined for *P*-values <0.05 . Statistical analysis was performed using the Statistical Package for Social Sciences, version 20.0 (IBM SPSS, Chicago, IL, USA).

RESULTS

Clinical Characteristics of Patients

We analyzed a total of 29 human hearts: 23 explanted human hearts from patients diagnosed with HF undergoing cardiac transplantation and six non-diseased donor hearts as CNT samples by RNA-Seq. All analyzed patients were men, except for one woman in the DCM group. The mean age of the patients was 54 ± 8 years. The patients had an NYHA functional classification of III–IV and had previously been diagnosed with significant comorbidities, including hypertension and hypercholesterolemia.

Table 1 shows the mean \pm s.d. of the clinical characteristics of the patients according to the etiology of HF. The ICM group had significantly larger values for EF ($P < 0.05$), and fractional shortening (FS; $P < 0.05$), and lower values for LV end-systolic diameter (LVESD; $P < 0.05$), LVEDD ($P < 0.05$), and LV mass (LVm; $P < 0.05$) compared with those in the DCM group.

The CNT group had a mean age of 53 ± 10 years.

RNA-Seq Results

To investigate the changes accompanying human HF, we performed a large-scale expression screen using RNA-Seq technology. A total of 29 heart samples were used for RNA-Seq analysis (ICM, $n = 13$; DCM, $n = 10$; and CNT, $n = 6$). Significance analysis of the RNA-Seq results revealed a total of 1334 genes that were differentially expressed in ICM patients *vs* CNT; 649 genes were upregulated (≥ 1.5 -fold, $P < 0.05$) and 685 genes were downregulated (≤ 1.5 -fold, $P < 0.05$). Additionally, 1628 genes were differentially expressed in DCM patients *vs* CNT; 596 genes were upregulated (≥ 1.5 -fold, $P < 0.05$) and 1032 genes were down-

regulated (≤ 1.5 -fold, $P < 0.05$). These genes make HF transcriptome signature. RNA-Seq data are available at GEO public resource and the accession number to the data file is GSE55296 (<http://www.ncbi.nlm.nih.gov/geo/query/acc.cgi?acc=GSE55296>).

Bioinformatic analysis of dysregulated genes identified in RNA-Seq analysis.

We next performed a functional analysis of the genes using the DAVID database. We analyzed GO terms enrichment in the Biological Process (BP) and Cellular Component (CC) categories of differentially expressed HF genes to identify functional processes of biological importance.

The functional annotation of the dysregulated genes revealed GO terms involved in cytoskeletal function such as cell adhesion, cell motion, muscle contraction, and regulation of heart contraction in patients with HF in both pathologies (Figure 1). We also identified 28 and 15 genes associated with actin-filament process and contractile fibers part, respectively, that were differentially represented only in ICM. Therefore, GO term analysis of our RNA-Seq data demonstrated that cytoskeletal processes are altered in HF.

Finally, using this bioinformatic approach and an extensive literature review, we identified a total of 60 candidate genes associated with the cytoskeleton in ICM and 58 genes involved in DCM (Supplementary Table S1). Up to 32 of these genes were shared in both diseases (Figure 2a). Among the identified differentially expressed genes, some had been previously associated with HF, such as *ACTA1*, *VCL*, *NEB*, and *MYH6*,^{21,22} as well as several collagen genes (*COL1A* or *COL3A*) upregulation. The deregulation of new thin filament and regulator genes were identified in this study, such as *TNNT3*, *TPM3*, tubulin genes (*TUBB2B*, *TUBA3E*), integrins (*ITGA3* or *ITGAE*), and regulators of the actin cytoskeleton (*ARHGEF6*, *RDN1*, or *MAPK10*).

On the other hand, we also investigated the behavior of the common cytoskeletal genes using hierarchical clustering analysis. As is shown in Figure 2b, both pathologies exhibited similar changes in these cytoskeletal genes. Clustering analysis identified three groups. Genes within cluster 2 were upregulated in HF and genes within cluster 3 were downregulated. Cluster 1 did not demonstrate a specific pattern relative to HF.

RNA-Seq Validation

To validate the results obtained by RNA-Seq analysis, qRT-PCR was performed. We selected the following three genes from the group of altered cytoskeletal components uniquely identified in this study: *MYLK4*, *RHOA*, and *ANKRD1*. These genes are closely involved in the regulation of the actin cytoskeleton and muscle contraction.

qRT-PCR analysis revealed decreased expression of *MYLK4* (-2.2 -fold, $P < 0.05$) at the mRNA level and increased expression of *ANKRD1* (2.3 -fold, $P < 0.01$) in ICM patients. *RHOA* mRNA levels exhibited a statistical trend of decrease (-2.9 -fold, $P = 0.07$) compared with CNT (Figure 3a).

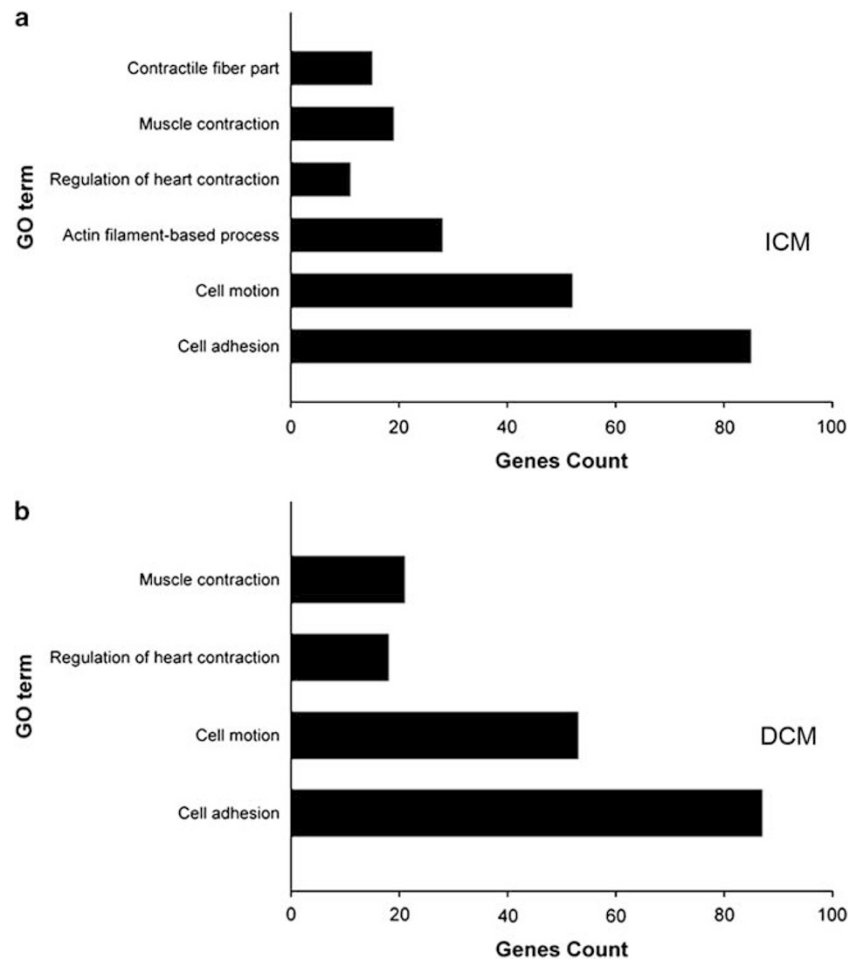


Figure 1 GO term enrichment analysis of dysregulated genes identified in RNA-Seq analysis. List of GO terms associated with cytoskeleton function identified using the DAVID functional annotation database, and the number of genes associated with each term. (a) ICM and (b) DCM patients. All comparisons were statistically significant ($P < 0.05$).

When we compared hearts from DCM patients with CNT hearts, we found that *MYLK4* (-4 -fold, $P < 0.05$) and *RHOU* (-3.9 -fold, $P < 0.05$) were downregulated and *ANKRD1* was upregulated (2.5 -fold, $P < 0.05$; Figure 3b).

Protein Level Analysis

To determine whether gene expression changes trigger changes in protein levels, we performed western blot analysis of *MYLK4*, *RHOU*, and *ANKRD1*. Western blot results showed that in ICM vs CNT LV samples *MYLK4* protein levels were decreased (67.6 ± 25.8 vs 100 ± 25.8 ; $P < 0.05$) and *ANKRD1* levels were increased (171.7 ± 59.7 vs 100 ± 37.6 ; $P < 0.05$; Figure 4). The same was obtained in DCM; *MYLK4* levels were decreased (64.5 ± 21 vs 100 ± 21.8 ; $P < 0.05$) and *ANKRD1* levels were increased (171.7 ± 71.7 vs 100 ± 37.6 ; $P < 0.05$) comparing with CNT samples (Figure 4). The results confirm that ICM and DCM patients display changes in *ANKRD1* and *MYLK4* gene and protein levels.

Furthermore, *RHOU* protein levels increased in ICM comparing with CNT (163 ± 55.6 vs 100 ± 14.9 ; $P < 0.05$) and

did not show statistically significant change in DCM comparing with CNT (114.9 ± 12.6 vs 100 ± 14.9 ; Figure 4).

Relationship between Changes in Gene Expression and LV function Parameters

In order to determine the clinical relevance of the dysregulated genes, we determined whether there were any correlations between gene expression levels (*MYLK4*, *RHOU*, *ANKRD1*) and LV function parameters in the whole HF population. *ANKRD1* was significantly related with FS ($r = 0.52$, $P < 0.05$; Figure 5a), and changes in *RHOU* expression were related with LV mass (LVm; $r = -0.60$, $P < 0.05$; Figure 5b).

DISCUSSION

HF is a syndrome in which the heart cannot pump enough blood to meet the needs of the body.¹ Cardiomyocyte cytoskeleton represents a key node maintaining cell morphology and regulating contraction/relaxation.^{5,23} Alterations in cytoskeletal components have been demonstrated in both animal models and humans in HF.^{9,24} It was proposed that an

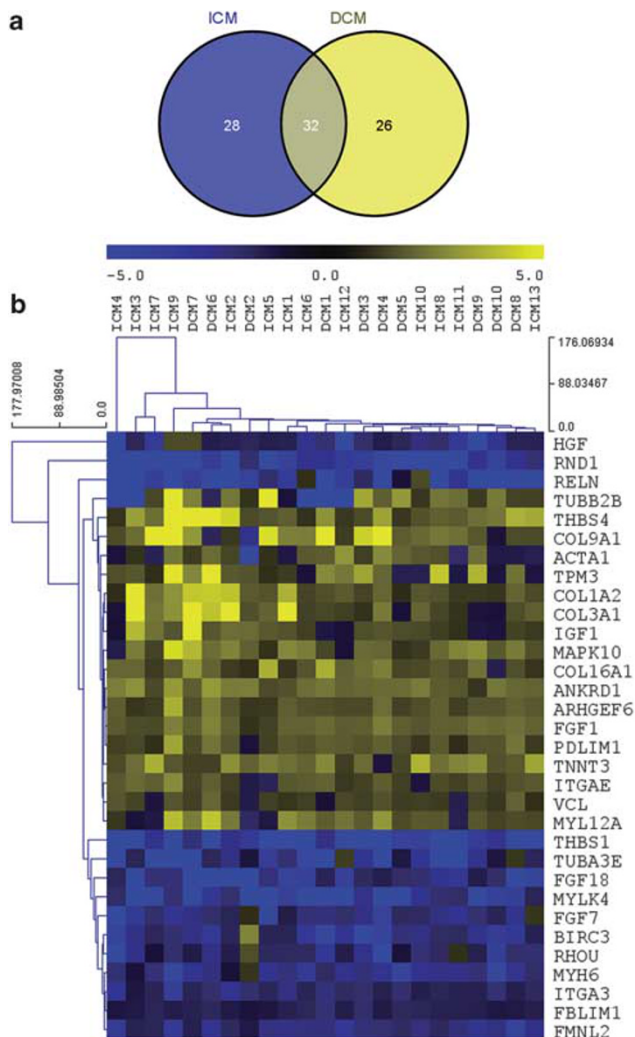


Figure 2 Altered gene expression associated with cytoskeletal function in HF. **(a)** Venn diagram showing the comparison of differentially expressed genes associated with cytoskeleton between ICM and DCM patients. **(b)** Expression levels of key cytoskeleton genes revealed by whole-transcriptome RNA-sequencing are shown in a heat map. The relative expression level of each gene is indicated by the color bar. Clustering analysis identified three groups.

increase in cytoskeletal membrane-associated proteins accompanied by loss of contractile filaments are the main changes that may be regarded as the morphological causes of heart dysfunction.^{25,26} Although the number of genes known to be involved in structural disruption in HF increases every year, a large number of cytoskeleton and effector genes were not discussed yet. Therefore, the objective of this study was to highlight a select group of cytoskeleton genes and effectors using RNA-Seq, comparing patients with ICM and non-ischemic DCM to CNT, and to find out their functional relationship.

Functional analysis of RNA-Seq results demonstrated that cytoskeletal processes are altered in HF and identified a total of 60 cytoskeleton-related genes differentially expressed in

ICM. When we compared hearts from DCM patients with CNT hearts, we found 58 differentially expressed cytoskeleton-related genes. Among the differentially expressed genes, some were previously associated with HF, such as *ACTA1*, *VCL*, *NEB*, and *MYH6*.^{21,22} Furthermore, the RNA-Seq results were consistent with data from previous studies. It is well described that the upregulation of collagen genes has been associated with the fibrosis process²⁷ and the increased expression of membrane-associated proteins, such as *VLC*,⁹ has an adaptive response to cellular integrity loss. We can also highlight the novel identification of altered expression of thin filaments and their regulator genes, such as *TNNT3*, *TPM3*, tubulin genes (*TUBB2B*, *TUBA3E*), integrins (*ITGA3* or *ITGAE*) implicated in focal adhesion and mechanical signaling, and regulators of the actin cytoskeleton (*ARHGEF6*, *RDN1*, and *MAPK10*).

Despite the different etiologies of ICM and DCM, both pathologies converge on similar functional changes, these shared alterations are responsible for HF. Therefore, in our work we focus on the behavior study of 32 differentially expressed genes shared in both pathologies using a hierarchical analysis of RNA-Seq data. Our results determined that both pathologies exhibit similar changes in these cytoskeletal genes, and therefore it was not possible to differentiate between ICM and DCM individual patients. Cytoskeletal gene changes at different etiologies of HF may be a common molecular key. It could be a case of shared transcriptional adaptation of the heart to different myocardial stress and injury focus. Furthermore, clustering analysis identified three main genetic patterns—genes that were upregulated, genes downregulated in HF and genes that did not demonstrate a specific pattern relative to HF.

To validate the RNA-Seq data, qRT-PCR analysis was performed on a greater number of samples (36 samples: 16 ICM, 13 DCM, 7 CNT). We selected two genes not previously associated with these cardiomyopathies, *RHO* and *MYLK4*. *ANKRD1* levels were previously analyzed in other studies but have not been characterized using next-generation technologies yet.²⁸ All these genes are closely associated with cytoskeletal process and muscle contraction regulation. Our results confirm the RNA-Seq analysis and determine a decreased mRNA expression of *RHO* and *MYLK4* and increased mRNA expression of *ANKRD1* in patients with DCM. In ICM patients we found that *MYLK4* was downregulated and *ANKRD1* was upregulated. *RHO* mRNA levels showed a statistical trend to decrease. Western blot analysis determined a decrease in *MYLK4* and increased *ANKRD1* protein levels in HF, reinforcing their relevance in the disease. *RHO* protein levels increased in ICM and did not show change in DCM comparing with CNT.

ANKRD1 is a transcription factor and interacts with the sarcomeric proteins acting in the myofibrillar stretch-sensor system. Overexpression and increased protein levels of *ANKRD1* in failing myocardium have been previously described, suggesting that this factor may significantly

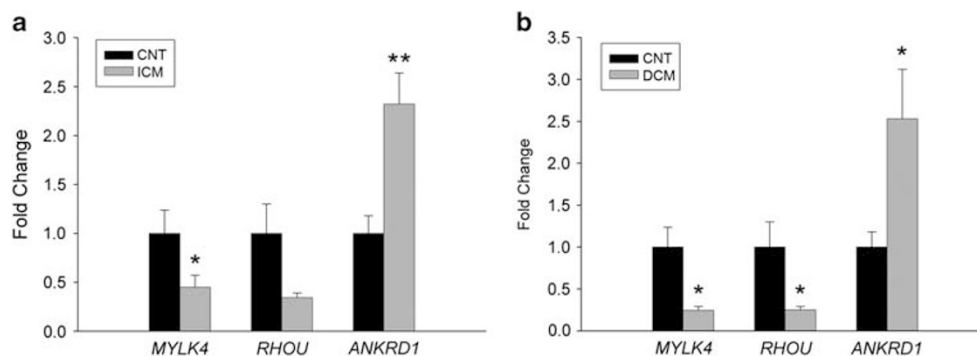


Figure 3 Expression levels of cytoskeleton genes. The differential expression of *MYLK4*, *ANKRD1*, and *RHO* was validated using qRT-PCR in ICM patients vs CNT (a) and DCM patients vs CNT (b). Results were considered statistically significant at * $P < 0.05$, ** $P < 0.01$. Bars represent means \pm s.e.m.

contribute to pathological heart remodeling.^{28,29} It is surprising, however, that most investigations have focused on the induction of *ANKRD1* expression in animal models and *in vitro* cultured primary cardiomyocytes. Thus, our study confirmed previous studies and provided accurate data about the increased *ANKRD1* levels in human HF samples. We also found a relationship between *ANKRD1* mRNA levels and FS demonstrating that *ANKRD1* upregulation is associated with altered systolic/diastolic function.

It is well known that muscle contraction and its molecular motor, myosin, are regulated through the phosphorylation of the regulatory myosin light chain (MLC2), mediated by myosin light-chain kinases (MLCK). MLC2 has a major role in regulating cardiac function, and therefore MLC2 phosphorylation status, regulated by MLCKs, is critical to this process.³⁰ Chan *et al* identified a new MLCK that is specifically expressed in the heart, MLCK3, or cardiac MLCK.³¹ The downregulation of cardiac MLCK decreases the steady-state levels of MLC2 phosphorylated; therefore, it was proposed to be the main myosin kinase acting on cardiac myocytes.^{31,32} Decreased levels of phosphorylated MLC2-P have been observed in HF.³³ In addition, these studies demonstrated a global decrease of myofilament protein phosphorylation occurring during HF. MLCK3 was also identified as a HF-related gene.³⁴ Surprisingly, studies in mice have demonstrated that the ablation of MLCK3 attenuates MLC2 phosphorylation and no changes in tissue morphology occur.³⁵ These data suggest that another kinase could phosphorylate MLC and could participate in the structural and functional changes that occur during HF. Recently, a new MLCK has been discovered, MLCK4 or MYLK4. Despite the importance of the myosin kinases in heart pathophysiology, there have been no studies of MLCK4 to date. Our study is the first report that demonstrates the expression of *MYLK4* in human hearts. Our results also reveal that patients with HF exhibit a significant decrease in *MYLK4* gene expression and protein levels. Given these data, further functional *MYLK4* studies may determine whether this myosin kinase is partially responsible for the decrease in myofilament phosphorylation levels during HF.

Another important gene differentially expressed in HF is *RHO*. *RHO* is a member of the Rho family of GTPases with atypical features that participates in the regulation of cell morphology and cytoskeletal organization.³⁶ Recent studies have found that *RHO* transient expression in NHT-3T3 cells disrupts stress fiber content.³⁷ Transcript levels of *RHO* were also found to be decreased in many tumor types relative to normal tissue.³⁸ *RHO* is hypothesized to maintain the cell architecture through F-actin polarization, and future studies will elucidate the exact mechanisms of this regulation.^{39,40} Another study reported that *RHO* downregulation diminishes F-actin distribution, reducing the resistance of epithelial cells to compressive force.⁴¹ Changes in *RHO* expression may also affect cardiomyocyte resistance to blood pressure overload or other mechanical forces that occur during HF.⁴² Our study demonstrates the downregulation of *RHO* expression in HF patients while increased protein levels only in ICM. These data are suggesting that gene translational regulatory mechanism could be acting in *RHO* regulation, specifically in increased mRNA stability. This change would enhance mRNA translation increasing *RHO* protein levels in ICM patients.

Given the role of *RHO* in cell morphology, these alterations could be responsible for the disruption of cell architecture in HF. Furthermore, and in accordance with this hypothesis, we found a strong relationship between *RHO* mRNA levels and the LVm in our patients.

A limitation of this study is that the use of cardiac tissues from end-stage failing human hearts are limited by the high variability in disease etiology and treatment. To make our study population etiologically homogeneous, we chose DCM patients who did not report any family history of the disease. Another issue is that the study was performed in heart tissues and not in isolated cardiomyocytes. However, our group has analyzed these samples using confocal and electron microscopy techniques. Images show that cardiomyocytes are the majority of the cell population. In addition, the patients included in this study were receiving conventional therapy, and certain treatments may influence the mRNA or protein level.

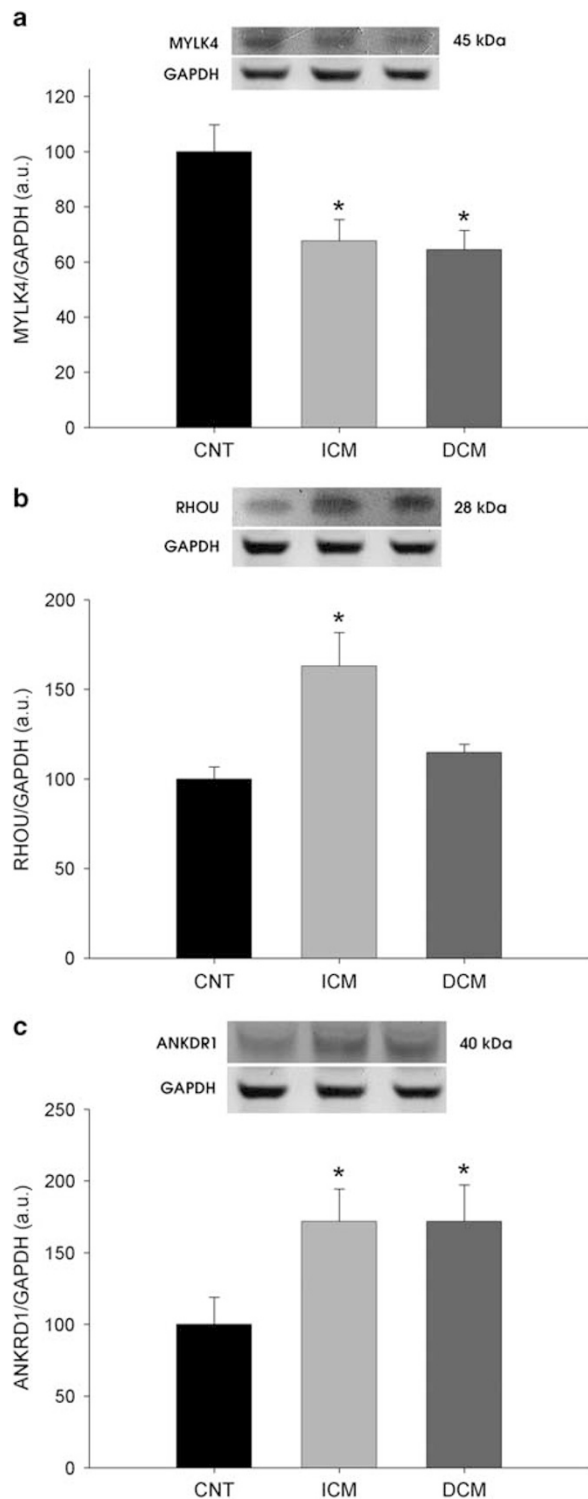


Figure 4 Cytoskeleton protein level analysis in HF patients. Representative western blot of MYLK4 (a), RHOU (b), and ANKRD1 (c) and GAPDH in the control in ICM and DCM. Quantification of protein levels are shown in the graph. Data represent the mean and error bars represent the s.e.m. Statistical analysis * $P < 0.05$ vs CNT.

In summary, RNA-Seq analysis of LV tissue revealed a new map of gene expression and protein changes in the ICM and DCM cardiomyocyte cytoskeleton. *MYLK4* and *RHOU*,

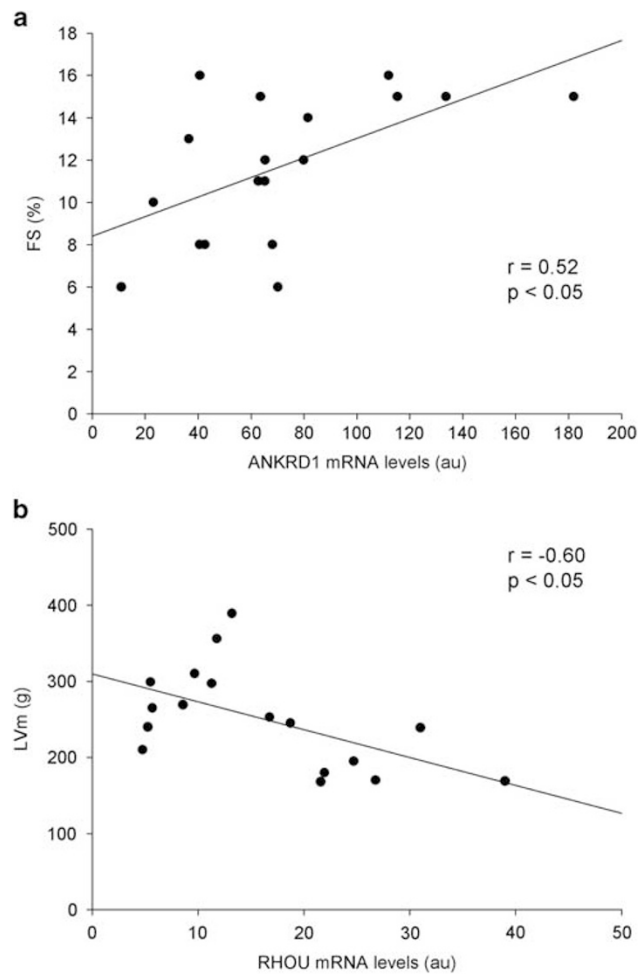


Figure 5 Relationship between gene expression levels and left ventricular function parameters of HF patients. (a) Fractional shortening (FS) vs ANKRD1 mRNA levels. (b) LV mass (LVm) vs RHOU mRNA levels. Arbitrary units (a.u.).

involved in crucial cellular mechanisms, were not previously implicated in the molecular phenotype of HF. Finally, *ANKRD1* and *RHOU* were related with changes in LV function. These new cytoskeletal changes may be responsible for altered contraction and cell architecture disruption in HF patients.

Supplementary Information accompanies the paper on the Laboratory Investigation website (<http://www.laboratoryinvestigation.org>)

ACKNOWLEDGMENTS

We thank the Transplant Coordination Unit (Hospital Universitario La Fe, Valencia, Spain) for their help in obtaining the heart tissue samples and Dr Jose Antonio Martínez Conejero for his valuable support. This work was supported by grants from the National Institute of Health 'Fondo de Investigaciones Sanitarias del Instituto de Salud Carlos III' (Retics RD12/0042/0003, and FIS Projects PI10/00275 and PI13/00100).

DISCLOSURE/CONFLICT OF INTEREST

The authors declare no conflict of interest.

1. Mann DL. Mechanisms and models in heart failure: a combinatorial approach. *Circulation* 1999;100:999–1008.
2. Cortés R, Rivera M, Roselló-Lletí E, *et al*. Differences in MEF2 and NFAT transcriptional pathways according to human heart failure aetiology. *PLoS One* 2012;7:e30915.
3. Kehat I, Molkentin JD. Molecular pathways underlying cardiac remodeling during pathophysiologic stimulation. *Circulation* 2010;122:2727–2735.
4. Heling A, Zimmermann R, Kostin S, *et al*. Increased expression of cytoskeletal, linkage, and extracellular proteins in failing human myocardium. *Circ Res* 2000;86:846–853.
5. Ruwhof C, van der Laarse A. Mechanical stress-induced cardiac hypertrophy: mechanisms and signal transduction pathways. *Cardiovasc Res* 2000;47:23–37.
6. Chien KR. Genomic circuits and the integrative biology of cardiac diseases. *Nature* 2000;407:227–232.
7. Kostin S, Hein S, Arnon E, *et al*. The cytoskeleton and related proteins in the human failing heart. *Heart Fail Rev* 2000;5:271–280.
8. Zile MR, Green R, Schuyler GT, *et al*. Cardiocyte cytoskeleton in patients with left ventricular pressure overload hypertrophy. *J Am Coll Cardiol* 2001;37:1080–1084.
9. Hein S, Kostin S, Heling A, *et al*. The role of the cytoskeleton in heart failure. *Cardiovasc Res* 2000;45:273–278.
10. Knöll R, Hoshijima M, Hoffman HM, *et al*. The cardiac mechanical stretch sensor machinery involves a Z disc complex that is defective in a subset of human dilated cardiomyopathy. *Cell* 2002;111:943–955.
11. Arber S, Hunter JJ, Ross Jr J, *et al*. MLP-deficient mice exhibit a disruption of cardiac cytoarchitectural organization, dilated cardiomyopathy, and heart failure. *Cell* 1997;88:393–403.
12. Shen YT, Malik FI, Zhao X, *et al*. Improvement of cardiac function by a cardiac Myosin activator in conscious dogs with systolic heart failure. *Circ Heart Fail* 2010;3:522–527.
13. Molina-Navarro MM, Roselló-Lletí E, Tarazón E, *et al*. Heart failure entails significant changes in human nucleocytoplasmic transport gene expression. *Int J Cardiol* 2013;168:2837–2843.
14. Grzeskowiak R, Witt H, Drungowski M, *et al*. Expression profiling of human idiopathic dilated cardiomyopathy. *Cardiovasc Res* 2003;59:400–411.
15. Yung CK, Halperin VL, Tomaselli GF, *et al*. Gene expression profiles in end-stage human idiopathic dilated cardiomyopathy: altered expression of apoptotic and cytoskeletal genes. *Genomics* 2004;83:281–297.
16. Mooney M, Bond J, Monks N, *et al*. Comparative RNA-Seq and microarray analysis of gene expression changes in B-cell lymphomas of *Canis familiaris*. *PLoS One* 2013;8:e61088.
17. Swedberg K, Cleland J, Dargie H, *et al*. Guidelines for the diagnosis and treatment of chronic heart failure: executive summary (update 2005): The Task Force for the Diagnosis and Treatment of Chronic Heart Failure of the European Society of Cardiology. *Eur Heart J* 2005;26:1115–1140.
18. Macrae DJ. The Council for International Organizations and Medical Sciences (CIOMS) guidelines on ethics of clinical trials. *Proc Am Thorac Soc* 2007;4:176–178.
19. Trapnell C, Williams BA, Pertea G, *et al*. Transcript assembly and quantification by RNA-Seq reveals unannotated transcripts and isoform switching during cell differentiation. *Nat Biotechnol* 2010;28:511–515.
20. Livak KJ, Schmittgen TD. Analysis of relative gene expression data using real-time quantitative PCR and the 2(-Delta Delta C(T)) Method. *Methods* 2001;25:402–408.
21. Gupta A, Gupta S, Young D, *et al*. Impairment of ultrastructure and cytoskeleton during progression of cardiac hypertrophy to heart failure. *Lab Invest* 2010;90:520–530.
22. McCain ML, Parker KK. Mechanotransduction: the role of mechanical stress, myocyte shape, and cytoskeletal architecture on cardiac function. *Pflugers Arch* 2011;462:89–104.
23. Crossman DJ, Ruygrok PN, Soeller C, *et al*. Changes in the organization of excitation-contraction coupling structures in failing human heart. *PLoS One* 2011;6:e17901.
24. Kim HK, Thu VT, Heo HJ, *et al*. Cardiac proteomic responses to ischemia-reperfusion injury and ischemic preconditioning. *Expert Rev Proteomics* 2011;8:241–261.
25. Monreal G, Nicholson LM, Han B, *et al*. Cytoskeletal remodeling of desmin is a more accurate measure of cardiac dysfunction than fibrosis or myocyte hypertrophy. *Life Sci* 2008;83:786–794.
26. Hein S, Scholz D, Fujitani N, *et al*. Altered expression of titin and contractile proteins in failing human myocardium. *J Mol Cell Cardiol* 1994;26:1291–1306.
27. Weber KT, Janicki JS, Shroff SG, *et al*. Collagen remodeling of the pressure-overloaded, hypertrophied nonhuman primate myocardium. *Circ Res* 1988;62:757–765.
28. Zolk O, Frohme M, Maurer A, *et al*. Cardiac ankyrin repeat protein, a negative regulator of cardiac gene expression, is augmented in human heart failure. *Biochem Biophys Res Commun* 2002;293:1377–1382.
29. Mikhailov AT, Torrado M. The enigmatic role of the ankyrin repeat domain 1 gene in heart development and disease. *Int J Dev Biol* 2008;52:811–821.
30. Davis JS, Hassanzadeh S, Winitzky S, *et al*. The overall pattern of cardiac contraction depends on a spatial gradient of myosin regulatory light chain phosphorylation. *Cell* 2001;107:631–641.
31. Chan JY, Takeda M, Briggs LE, *et al*. Identification of cardiac-specific myosin light chain kinase. *Circ Res* 2008;102:571–580.
32. Sheikh F, Ouyang K, Campbell SG, *et al*. Mouse and computational models link Mlc2v dephosphorylation to altered myosin kinetics in early cardiac disease. *J Clin Invest* 2012;122:1209–1221.
33. Ishikawa Y, Kurotani R. Cardiac myosin light chain kinase: a new player in the regulation of myosin light chain in the heart. *Circ Res* 2008;102:516–518.
34. Hamdani N, Borbély A, Veenstra SP, *et al*. More severe cellular phenotype in human idiopathic dilated cardiomyopathy compared to ischemic heart disease. *J Muscle Res Cell Motil* 2010;31:289–301.
35. Asakura M, Kitakaze M. Global gene expression profiling in the failing myocardium. *Circ J* 2009;73:1568–1576.
36. Chang AN, Huang J, Battiprolu PK, *et al*. The effects of neuregulin on cardiac Myosin light chain kinase gene-ablated hearts. *PLoS One* 2013;8:e66720.
37. Ruusala A, Aspenström P. The atypical Rho GTPase Wrch1 collaborates with the nonreceptor tyrosine kinases Pyk2 and Src in regulating cytoskeletal dynamics. *Mol Cell Biol* 2008;28:1802–1814.
38. Saras J, Wollberg P, Aspenström P. Wrch1 is a GTPase-deficient Cdc42-like protein with unusual binding characteristics and cellular effect. *Exp Cell Res* 2004;299:356–369.
39. Bhavsar PJ, Infante E, Khwaja A, *et al*. Analysis of Rho GTPase expression in T-ALL identifies RhoU as a target for Notch involved in T-ALL cell migration. *Oncogene* 2013;32:198–208.
40. Loebel DA, Studdert JB, Power M, *et al*. Rho maintains the epithelial architecture and facilitates differentiation of the foregut endoderm. *Development* 2011;138:4511–4522.
41. Loebel DA, Tam PP. Rho GTPases in endoderm development and differentiation. *Small GTPases* 2012;3:40–44.
42. Sheehy SP, Grosberg A, Parker KK. The contribution of cellular mechanotransduction to cardiomyocyte form and function. *Biomech Model Mechanobiol* 2012;11:1227–1239.